Effect of prepreg storage humidity on the mixed-mode fracture toughness of a co-cured composite joint

J. Mohan[a], A. Ivanković[a], N. Murphy[a]

[a] *UCD Centre of Adhesion and Adhesives,*
School of Mechanical & Materials Engineering, University College Dublin, Belfield, Dublin 4, Ireland.
Tel: +353 (0)1 716 1880, Fax: +353 (0)1 283 534.

Abstract

The present work investigated the effect of the level of prepreg moisture content on the mixed-mode fracture toughness of a co-cured composite joint. It was found that moisture was stored in the prepreg as either free or bound water. It was also shown that the prepreg stores moisture from high humidity environments as free water, while the level of bound water remains unaffected. The excessive moisture was shown to plasticise the adhesive, lowering the glass transition temperature. The fracture toughness decreased under mode I and mode II loading as the humidity level was increased. The mixed-mode toughness also reduced with increasing storage humidity. However, the measured mixed-mode fracture toughness never reduced below that of the joints fabricated using the as-received material. This indicates that the moisture has a more pronounced effect on the bulk properties of the adhesive rather than on the interfacial adhesion between the composite and adhesive.

Keywords: A: prepreg, B: adhesion, B: fracture toughness, D: Thermal analysis

1. Introduction

Moisture represents one of the most aggressive damage mechanisms an adhesive joint can experience. Water can be introduced into the joint in a number of ways. It can be present in the composite substrate or prepreg prior to curing or co-curing [1]. If proper precautions are not met, condensation can form on the prepreg or adhesive when taken out of cold storage. Finally, it may enter the joint during in-service conditions [2, 3].

The role of moisture in composite joints is only recently being understood. In a series of tests to determine the effect of substrate material and test geometry on the mode I fracture toughness of adhesively bonded joints, Bell and Kinloch [4] found that the double cantilever beam (DCB) joints prepared with the composite substrates exhibited a much lower fracture toughness than those bonded with metallic substrates. These differences were initially believed to be due to the different levels of constraint in the various joint

Email address: joseph.mohan@ucd.ie (J. Mohan)

systems. In a later investigation [5], it was revealed that the differences were in fact caused by moisture stored in the composite substrate that was then released during the curing of the adhesive. These results were also published as part of a European Structural Integrity Society - Technical Committee 4 (ESIS-TC4) round-robin in the standardisation of adhesive fracture testing [6]. The same authors then undertook a more extensive investigation of the effect of pre-bond moisture in secondary bonded composite joints [1].

Once moisture has entered the joint, the effects can be quite complex and difficult to analyse. Small amounts of moisture, less that 1 %, can drastically reduce the fracture toughness of some adhesive joint systems [5, 1] while other systems can actually experience a slight increase in fracture toughness [2] that some attribute to extra energy being absorbed due to plasticisation of the adhesive [7]. It has also been shown that certain adhesives are relatively unaffected by small amounts of moisture, particularly film adhesives [8, 9, 1]. The deleterious effects of moisture in the adhesive can even be reversed through desorption [10].

A considerable amount of research has been published on the nature of water in epoxies that are used as neat resins, adhesives and in polymer composites. Water is stored in polymers in one of two states; free water (type I) or bound water (type II) [11]. Type I free water disrupts the initial interchain Van der Waals forces and hydrogen bonds resulting in increased chain segment mobility. Type II bound water forms multiple hydrogen bonds with the polymer network. Therefore, type I free water acts as a plasticizer and decreases the glass transition temperature, T_g, [12] while type II bound water acts as a secondary crosslinked network and can increase T_g [12, 13]. Berry et al. [13] reported a similar effect of absorbed moisture in a rubber modified epoxy. In that work, small amounts of moisture were found to increase the glass transition temperature due to the formation of strong dipole-dipole interactions. However, further levels of absorption decreased T_g. Others have estimated the amount of residual bound water that remains in epoxy resins after drying, having previously been stored in a hot/wet environment, as being approximately 0.12% [14]. In order to remove this remaining water, an activation energy of the order of 6 kcal/mol is required. The authors noted that this is very close to the activation energy of a hydrogen bond.

Referring back to the work of Zhou and Lucas [11], the authors noted that the water from hot/wet environments was typically absorbed by the epoxy as free water. The level of type II bound water only increased significantly when the samples were stored for very long times at elevated temperatures in the hot/wet environments. The apparent reluctance of the water to be stored as bound water within the polymer network may be due to the higher activation energy needed to form the required hydrogen bonds. It is possible that the bound water was introduced into the epoxy resin during the manufacturing process. Polymer matrices used in the manufacture of composite materials consist of epoxy resins, thermoplastic tougheners and curing agents. These constituent components are typically mixed at elevated temperatures. The high temperature could provide enough energy to form multiple hydrogen bonds between the polymer network and any water present. While free water can always be removed by drying the polymer, in order to prevent the absorption of bound water, every stage of the manufacturing process would have to be strictly

controlled.

Work has also been published on the effects of moisture on bulk adhesive specimens before and after cure. Hartwig [15] investigated the effect of humidity on the crosslinking of a photocured epoxy resin. The authors reported that the environments with higher humidity retarded the crosslinking of the epoxy end-groups, perhaps due to the disruption of the initial interchain Van der Waals forces and hydrogen bonds as discussed above. LaPlante and Lee-Sullivan [9] investigated the effect of moisture on the mechanical properties of FM300-1K film adhesive (the high temperature cure version of the adhesive used in the present study). In that work, bulk single edged notched specimens were aged in various humid environments and then tested in three point bending. The authors reported an increase in toughness of the samples aged in each humid environments compared to the as-received specimens. The authors also attributed this increase in toughness to higher levels of energy absorption due to plasticisation of the adhesive.

The aim of the present work is to investigate the effects of prepreg moisture content on the mode I, mode II and mixed-mode fracture toughness of a co-cured composite joint.

2. Materials & manufacture of joints

Two aerospace grade materials were used in the present study; a 180 °C cure unidirectional carbon-fibre/epoxy prepreg (CYCOM 977-2/HTS) and a dual 120/180 °C cure epoxy film adhesive (FM300-2M). The film adhesive contains a polyester scrim cloth with random fibre orientation that aids in handling and also in controlling the bondline thickness. Both materials were manufactured and supplied by Cytec Engineered Materials (CEM).

The composite laminates and adhesive joints were produced in-house at UCD using a vacuum bagging layup procedure similar to that used in industry. Co-cured joints were produced by curing the prepreg and the adhesive at the same time. A 20 ply prepreg layup was prepared with a sheet of film adhesive between the 10^{th} and 11^{th} ply to produce a symmetrically cracked specimen. A 12 μm thick PTFE sheet was used as a crack initiator. The prepreg and adhesive were then cured at 180 °C to produce a co-cured composite joint.

Once cured, the bonded composite laminates were machined to size using a diamond grinding disc. The specimens were cut to a nominal width of 25 mm and length of either 150 mm (for mode I tests) or 190 mm (for mode II/mixed-mode tests) with an initial crack starter length of 45 mm (mode I) or 65 mm (mode II/mixed-mode) from the load-line. The total thickness of each specimen was $\approx$5.6 mm with an adhesive layer thickness of $\approx$0.25 mm as controlled by the scrim cloth.

3. Experimental methods

3.1. Fracture test methods

Mode I double cantilever beam (DCB) tests were conducted in accordance with the British Standard outlined in [16]. The mode II end-loaded split (ELS) test used the latest revision of the ESIS-TC4 protocol [17]. The fixed-ratio mixed-mode (FRMM) test used the provisional protocol in [18] as well as several papers by Williams [19, 20, 21] as a guideline.

An illustration of the DCB specimen, with key components highlighted, can be seen in Figure 1a. The FRMM and ELS tests utilised a fixture that clamped one end of the specimen such that it was fixed in the vertical (or y) direction but free to slide in the horizontal (or x) direction as can be seen in Figures 2 and 3. A Tinius-Olsen Hounsfield 50K screw-driven tensile test machine was used for the fracture tests. A 10 kN load cell was used to record the applied load. The crack length was monitored using a travelling microscope with $\times 10$ magnification. All tests were carried out at a constant crosshead displacement rate of 1 mm/min at room temperature. The specimens were held in place using load shackles and loading pins as shown in Figure 1b. Three repeats were performed for each test condition.

The propagation fracture toughness, G_C, was calculated using a corrected beam theory (CBT) analysis from Equation (1) for the DCB test, Equation (2) for the ELS test and Equation (3) for the FRMM test.

$$G_{IC} = \frac{3P\delta}{2B(a+|\Delta_I|)}.\frac{F}{N} \tag{1}$$

$$G_{IIC} = \frac{9P^2\left(a+|\Delta_{II}|\right)^2}{4B^2h^3E_f}.F \tag{2}$$

$$G_{I/IIC} = G_I + G_{II} \tag{3a}$$

$$G_I = \frac{3P^2\left(a+|\Delta_I|\right)^2}{B^2E_fh^3}.F \tag{3b}$$

$$G_{II} = \frac{9P^2\left(a+|\Delta_{II}|\right)^2}{4B^2E_fh^3}.F \tag{3c}$$

where P is the load, δ the opening displacement, B the width of the specimen, h the thickness of the beam, E_f the flexural modulus and a the crack length. F, N and Δ_I/Δ_{II} are correction factors for large displacements, load block effects and root rotation of the crack tip respectively and are based on several papers by Williams [19, 20, 21] and are detailed in [16], [17] and [22].

A total of 3 mode-mixities were examined and each test will be referred to by the following designations:

- DCB - Pure Mode I
- FRMM - Mixed-mode I/II (57% mode I/43% mode II)
- ELS - Pure Mode II

3.2. Humidity control

The investigation into the effect of prepreg storage humidity on the fracture toughness of co-cured joints was conducted using humidity controlled environments (i.e. an air tight container). The humidity was controlled using saturated salt solutions. Four different salt solutions were used. Table 1 details the salts used and the relative humidities they provide [23]. The larger sheets of prepreg were conditioned in a desiccator while the smaller samples used for systematic gravimetric analysis were stored in polypropylene boxes with a rubber seal.

3.3. Thermal characterisation methods

Thermal characterisation was performed on a Rheometric Scientific STA 1500. This apparatus is capable of performing both differential thermal analysis (DTA) and thermogravimetric analysis (TGA). Small samples of material ($\approx$ 20-30 mg) were placed in a 6 mm diameter aluminium crucible. An empty crucible was used as a reference sample for DTA. The samples were kept in a flowing nitrogen atmosphere throughout the analysis.

Two different types of heating regimes, dynamic scans and simulated cure cycles, were used on the adhesive and prepreg materials. Dynamic scans were used to determine the glass transition temperature of the adhesive. Simulated cure cycles were used to determine the weight loss of the prepreg over the course of a cure cycle. During dynamic scans, the sample was heated from 25 °C to 350 °C at a rate of 10 °C/min. During simulated cure cycles, the sample was heated from 25 °C to 180 °C at a rate of 1.5 °C/min and then held at 180 °C for 2 hrs.

A simulated cure cycle was also performed on a prepreg sample using a Thermal Analysis (TA) TGA Q500 with a Hiden Analytical HPR20 mass spectrometer (MS) gas flow analyser. During the heating regime, water was released over the course of the cure cycle and monitored (note that water has a mass to charge, m/z, ratio of 18). Figure 4 shows a rise in the intensity of water at the beginning the cure cycle representing the release of free water from the prepreg and again at 180 °C when the bound water is released.

3.4. Microscopy methods

Optical microscopy (OM) was performed using an Olympus GX51 Inverted Optical Microscope. After a fracture test, sections were cut from the sample. These sections were then set in a polymer mounting agent such that the longitudinal section through the joint was visible. The samples were then ground and polished to a smooth surface finish. Figure 5 shows a typical image from such a sample. The composite substrates can be seen at the top and bottom of the micrograph as well as regions corresponding to interfacial and cohesive failure. The polymer mounting agent can be seen in the centre of the micrograph and should be ignored.

Scanning electron microscopy (SEM) was performed on the resulting fracture surfaces using a Hitachi TM-1000 Tabletop Microscope. The TM-1000 uses a backscattered electron (BSE) detector and can provide images up to ×10,000 magnification. Samples were gold coated prior to imaging to reduce charging.

4. Results & discussion

4.1. Gravimetric & Thermogravimetric Analysis

A Mettler AE260 DeltaRange microbalance with a resolution of 0.0001 g was used to monitor the change in weight of the prepreg in the different humid environments. Samples of prepreg were stored in the smaller desiccators for a period of 308 days. Figure 6 shows a plot of change in weight versus the square root of storage time. It is interesting to note two distinct plateau regions in the Figure. The first occurs after approximately 3 to 4 days. The second plateau occurs towards the end of the 308 day period, particularly for the samples stored at 75% and 98% relative humidity. After the shelf life of the prepreg (28 days) has been reached the material becomes considerably more brittle and loses nearly all of its tack due to partial curing. It is interesting to note the second plateau region begins after the shelf life of the prepreg has been reached.

For consistency the prepreg sheets for co-curing were conditioned for a fixed time of 7 days in the larger desiccator. This time was chosen for two reasons. Firstly, the prepreg had reached a relatively stable level of moisture absorption after 7 days (see Figure 6). Secondly, the prepreg material remained in a workable condition after this amount of time (i.e. it retained reasonable flexibility and tack). The typical moisture absorption/desorption characteristics for the prepreg conditioned at the various humidity levels for 7 days are shown in Figure 7. While the adhesive likely also contains both free and bound water, it was decided to use the adhesive in the as-received conditions for all co-cured joints produced in this particular study. The reason for this was that 7 days represents only 25% of the shelf life of the prepreg but 70% of that of the adhesive (10 days). After this period of time, the film adhesive becomes noticeably brittle and retains little tack.

After conditioning in the humidity-controlled environments, the weight loss of the prepreg was monitored using a simulated cure cycle on the STA1500 system. Figure 8 shows a representative weight loss trace for the prepreg at the different humidities. The two distinct weight loss regions corresponding to free and bound water can be clearly seen. The quantities associated with free and bound water are shown in Figures 9a and 9b respectively. It appears that as the humidity level increases, the weight loss associated with free water also increases while the level of bound water remains relatively unaffected by humidity levels. Any differences in the levels of bound water are likely the result of variations in the prepreg material itself (e.g. changes in percentage content of resin).

The results of the associated fracture toughness tests will be presented in the next Section. However, the results for the glass transition temperature of the adhesive scrapings taken from the fracture surfaces will be presented now in the context of the other thermal analysis data. Figure 10 shows the results of T_g from the co-cured joints fabricated using RH conditioned prepreg. As the percentage humidity increases, there is a corresponding reduction in T_g. Even though the adhesive is a dual cure material for use with co-cure applications with 120 or 180 °C prepregs, it will still begin to cure at 120 °C as can be seen from the thermograph in Figure 11 (note the adhesive exothermic peak at approximately 80 min cure time). However, before the adhesive is fully cured, the free water stored in the prepreg is released and likely plasticises the adhesive as noted by Zhou and Lucas [12]. Dynamic scans on adhesive taken from the humidity conditioned co-cured joints revealed little difference in levels of residual cure, indicating the adhesive has been plasticised as opposed to not being fully cured.

4.2. Fracture toughness results

Co-cured joints prepared with the as-received (As-R) and RH conditioned prepreg were tested using the DCB, FRMM and ELS specimen geometries. The propagation fracture toughness, G_C, for each test can be found in Figure 12.

The results highlight some interesting points. Firstly, the mode I toughness decreases from approximately 900 J/m^2 in the As-R state to 700 J/m^2 when conditioned at 98% RH. Secondly, the mixed-mode toughness determined from the FRMM test shows an initial increase in G_C compared to the As-R specimens when conditioned at low humidities. However, the high humidity environments do not reduce the mixed-mode toughness below that of the samples fabricated using the As-R prepreg. Finally, there was a dramatic reduction in the mode II fracture toughness, G_{IIC}, as humidity levels increased.

Visual inspection of the fracture surfaces reveals another interesting point. While the locus of failure was primarily interfacial in nature for the as-received co-cured joint system, as humidity levels increased, there was a noticeable increase in the degree of cohesive failure at the higher humidity levels for the DCB (Figure 13) and ELS (Figure 15) geometries. This change was less evident for the FRMM geometries (Figure 14) where interfacial predominates for all humidity levels. This is in contrast to what is reported in the literature. Typically, the presence of moisture at an adhesive-substrate interface would cause the work of adhesion to become negative and displace the adhesive bond, resulting in interfacial failure [24]. A more recent example of this behaviour has been reported by Mubashar et al. [10]. In that work, aluminium joints bonded with FM73 film adhesive were aged in a hot/wet environment after bonding. The joints resulted in interfacial failure having previously exhibited cohesive failure before ageing.

The glass transition temperature results from Figure 10 show that the adhesive has been plasticised by the excess free water released during the co-curing process. This may, in turn, have a large effect on the energy absorption capacity of the adhesive. The dramatic reduction in mode II fracture toughness with

increasing percentage RH suggests this was indeed the case. The plasticised adhesive may also encourage a greater level of cohesive failure. The cohesive strength of the bulk plasticised adhesive may have reduced to near, or even below, that of the interfacial strength.

4.3. Microscopy Analysis

Figures 16, 17 and 18 show the crack paths at each RH for the DCB, FRMM and ELS specimen geometries respectively. For the DCB and FRMM tests, there was no noticeable difference in the profile of the crack paths. On the contrary, visual inspection of the fracture surfaces clearly showed an increase in the degree of cohesive failure (e.g. Figure 13). This was likely due to the fact that the micrographs are highly dependent on the location from which the cross section of the specimen is cut. However, the crack path during the mode II ELS test exhibits a significant change with increasing storage humidity levels. The extent of the larger 45° cracks that develop along the planes of maximum tensile principal stress during mode II fracture appears to be diminished as RH levels increase and the fracture surface associated with 98% is relatively flat.

To gain further insight into the changes observed during mode II fracture, SEM images were taken of the ELS fracture surfaces conditioned at 11% and 98% RH. The corresponding micrographs can be found in Figures 19 and 20 respectively. At the lower magnifications (×200), there seems to be little difference in the fracture surfaces. Contrary to the reduced number of large 45° cracks observed with optical microscopy, the amount of smaller 45° cracks that develop around the scrim cloth fibres appears to remain constant. It is only at the higher magnifications (×5000) that differences can be seen. The plasticisation caused by the elevated humidity levels lead to a more jagged fracture surface compared to that conditioned at 11% RH.

The results for the FRMM test show a rise in fracture toughness of approximately 20% at low humidity levels compared to the as-received specimens but then a steady decrease in toughness with increasing levels of humidity. However, the toughness never reduces below that of the co-cured joints produced using the as-received material. Cross-sections of the adhesive-substrate interface were taken from each co-cured joint conditioned at the various humidity levels and examined under SEM. Figure 21 shows the resulting micrographs. The joints fabricated using prepreg conditioned at 75% and 98% RH show an increase in the number, size and concentration of voids at the adhesive-substrate interface and, to a lesser extent, throughout the bulk adhesive. This weakened interface would explain the reduction in fracture toughness with increasing humidity levels presented in Figure 12b. However, this does not explain why the fracture toughness never falls below that of the as-received joint. Since the crack propagates along the interface under mixed-mode loading conditions, it is possible that the mixed-mode toughness of a co-cured joint is governed by the bond strength between the substrate and adhesive with less contribution from damage in the adhesive layer.

5. Conclusions

The fracture behaviour of the co-cured joint was greatly influenced by the free and bound water stored in the prepreg. This moisture was released during the co-curing cycle which then plasticised the adhesive and also resulted in primarily interfacial failure. The free water could be removed by drying the prepreg. However, the bound water could only be released by heating to 180 °C. The level of free water was found to be proportional to storage humidity while the bound water remained relatively constant.

The effect of the moisture content in the prepreg had very different effects depending on the test method employed. During mode I loading conditions, a reduction in fracture toughness of approximately 20% was observed at the highest humidity level compared to the joints fabricated using the as-received materials. The mode II toughness resulted in a much larger reduction of approximately 50% at 98% RH compared to the as-received joints. Optical and scanning electron microscopy suggest this was due to a reduction in energy absorption mechanisms such as the larger 45° cracks. The mixed-mode toughness determined using the FRMM geometry also exhibited a trend of decreasing fracture toughness with increasing RH. However, the measured toughness never reduced below that of the as-received materials. This was attributed to the fact that the interfacial fracture toughness was governed by the energy absorption mechanisms associated with the voids at the adhesive-substrate interface as opposed those in the bulk adhesive (e.g. large 45° crack formation during mode II loading).

Acknowledgements

The author's would like to gratefully acknowledge the financial support of the Irish Research Council for Science, Engineering and Technology (IRCSET) and Cytec Engineered Materials (CEM). The materials provided by CEM are also gratefully acknowledged.

References

[1] Blackman BRK, Johnsen BB, Kinloch AJ, Teo WS. The effects of pre-bond moisture on the fracture behaviour of adhesively-bonded composite joints. Journal of Adhesion 2008;84:256–76.

[2] Armstrong KB. Effect of absorbed water in CFRP composites on adhesive bonding. International Journal of Adhesion and Adhesives 1996;16:21–8.

[3] Woo RSC, Chen Y, Zhu H, Li J, Kim JK, Leung CKY. Environmental degradation of epoxy-organoclay nanocomposites due to UV exposure. part i: Photo-degradation. Composite Science and Technology 2007;67:3448–56.

[4] Bell AJ, Kinloch AJ. The effect of the substrate material on the value of the adhesive fracture energy, G_C. Journal of Material Science Letters 1997;16:1450–3.

[5] Blackman BRK, Kinloch AJ, Paraschi M. The effect of the substrate material on the value of the adhesive fracture energy, G_C: Further considerations. Journal of Material Science Letters 2001;20:265–7.

[6] Blackman BRK, Kinloch AJ, Paraschi M, Teo WS. Measuring the mode I adhesive fracture energy, G_{IC}, of structural adhesive joints: the results of an international round-robin. International Journal of Adhesion and Adhesives 2003;23:293–305.

[7] Halliday ST, Banks WM, Pethrick RA. Dielectric studies of adhesively bonded CFRP/epoxy/CFRP structures - design for ageing. Composites Science and Technology 2000;60:197–207.

[8] Kohli DK. Improved 121°C curing epoxy film adhesive for composite bonding and repair applications: FM300-2 adhesive system. International Journal of Adhesion and Adhesives 1999;19:231–42.

[9] LaPlante G, Lee-Sullivan P. Moisture effects on FM300 structural film adhesive: Stress relaxation, fracture toughness, and dynamic mechanical analysis. Journal of Applied Polymer Science 2005;95:1285–94.

[10] Mubashar A, Ashcroft IA, Critchlow GW, Crocombe AD. Moisture absorption-desorption effects in adhesive joints. International Journal of Adhesion and Adhesives 2009;29(8):751–60.

[11] Zhou J, Lucas JP. Hygrothermal effects of epoxy resin. Part I: the nature of water in epoxy. Polymer 1999;40:5505–12.

[12] Zhou J, Lucas JP. Hygrothermal effects of epoxy resin. Part II: variations of glass transition temperature. Polymer 1999;40:5513–22.

[13] Berry NG, dAlmeida JRM, Barcia FL, Soares BG. Effect of water absorption on the thermalmechanical properties of HTPB modified dgeba-based epoxy systems. Polymer Testing 2007;26:262–7.

[14] Lin YC, Chen X. Investigation of moisture diffusion in epoxy system: Experiments and molecular dynamics simulations. Chemical Physics Letters 2005;412:322–6.

[15] Hartwig A. Influence of moisture present during polymerisation on the properties of a photocured epoxy resin. International Journal of Adhesion and Adhesives 2002;22:409–14.

[16] BS-7991-2001 . Determination of the mode I adhesive fracture energy, G_{IC}, of structural adhesives using the double cantilever beam (DCB) and tapered double cantilever beam (TDCB) specimens. 2001.

[17] ESIS-TC4 . Fibre-composites - the determination of the mode II fracture resistance, G_{IIC}, of unidirectional fibre-composites using the calibrated end loaded split (C-ELS) test and an effective crack length approach. 2008.

[18] Blackman BRK, Brunner AJ, Davies P. Delamination fracture of continuous fibre composites: Mixed-mode fracture. In: Moore D, Pavan A, Williams J, editors. Fracture Mechanics Testing Methods for Polymers, Adhesives and Composites. Amsterdam: Elsevier Science; 2001, p. 335 –59.

[19] Williams JG. On the calculation of energy release rates for cracked laminates. International Journal of Fracture 1988;36:101–19.

[20] Williams JG. The fracture mechanics of delamination tests. Journal of strain analysis 1989;24(4):207–14.

[21] Hashemi S, Kinloch AJ, Williams JG. The analysis of interlaminar fracture in uniaxial fibre-polymer composites. Proceedings of the Royal Society of London 1990;427:173–99.

[22] Mohan J. An investigation of composite-to-composite bonding. Ph.D. thesis; University College Dublin; 2010.

[23] O'Brien FEM. The control of humidity by saturated salt solutions. Journal of Scientific Instruments 1948;25:73–6.

[24] Blackman BRK. The fracture behaviour of bonded polymeric fibre-composites. Ph.D. thesis; Imperial College London; 1993.

List of Tables

1 Salt solutions used in present study showing solubility in water and corresponding relative humidity [23]. 14

Salt	Solubility [g/100 ml]	RH [%]
Lithium Chloride (LiCl)	67	11
Potassium Carbonate (K_2CO_3)	112	43
Sodium Chloride (NaCl)	35	75
Potassium Sulphate (K_2SO_4)	11	98

Table 1: Salt solutions used in present study showing solubility in water and corresponding relative humidity [23].

List of Figures

1 Illustrations and photographs of DCB experimental setups showing loading directions and fixtures used during testing. . . . 16
2 Illustrations and photographs of FRMM experimental setups showing loading directions and fixtures used during testing. . . . 17
3 Illustrations and photographs of ELS experimental setups showing loading directions and fixtures used during testing. . . . 18
4 TGA-MS of water released from prepreg during the course of a cure cycle. . . . 19
5 A typical sample prepared for optical microscopy after fracture testing. . . . 19
6 Weight variation of prepreg stored at various humidities over the course of 308 days. The points corresponding to 7 days (conditioning time before co-curing) and 28 days (shelf life of prepreg) are highlighted. . . . 20
7 Weight variation of prepreg after 7 days at various humidity levels. . . . 20
8 Weight loss trace of prepreg stored at various humidity levels during a simulated 180 °C cure cycle. . . . 21
9 Percentage of free and bound water stored in the prepreg as determined by TGA. . . . 22
10 T_g of adhesive scrapings taken from fracture surface of co-cured joints. . . . 22
11 Heat flow of prepreg and adhesive over the course of a cure cycle. . . . 23
12 Fracture toughness of RH conditioned co-cured joints tested using DCB, FRMM & ELS geometries. . . . 24
13 Fracture surfaces of Mode I DCB test. . . . 25
14 Fracture surfaces of Mixed Mode FRMM test. . . . 26
15 Fracture surfaces of Mode II ELS test. . . . 27
16 Crack path for RH conditioned co-cured joints tested using DCB. . . . 27
17 Crack path for RH conditioned co-cured joints tested using FRMM. . . . 28
18 Crack path for RH conditioned co-cured joints tested using ELS. . . . 28
19 SEM image of fracture surface of co-cured joint conditioned at 11% RH and tested under mode II loading. . . . 29
20 SEM image of fracture surface of co-cured joint conditioned at 98% RH and tested under mode II loading. . . . 29
21 SEM images of adhesive-substrate interface of co-cured joints manufactured from prepreg aged at various humidities for 1 week. . . . 30

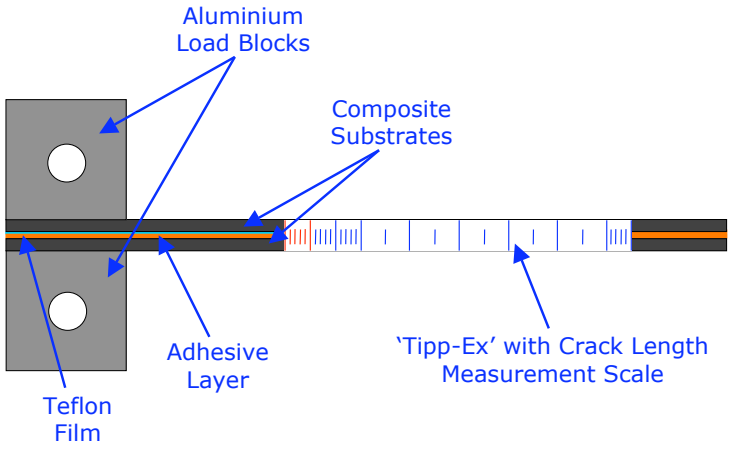

(a) DCB illustration.

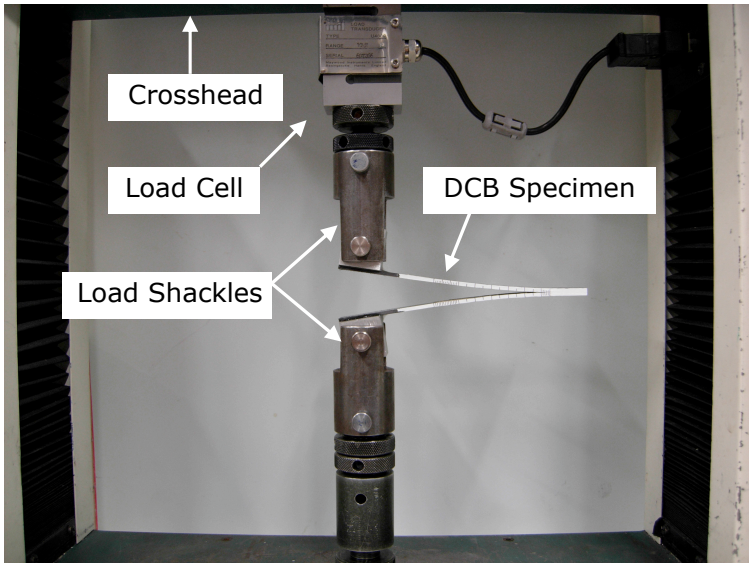

(b) DCB photo.

Figure 1: Illustrations and photographs of DCB experimental setups showing loading directions and fixtures used during testing.

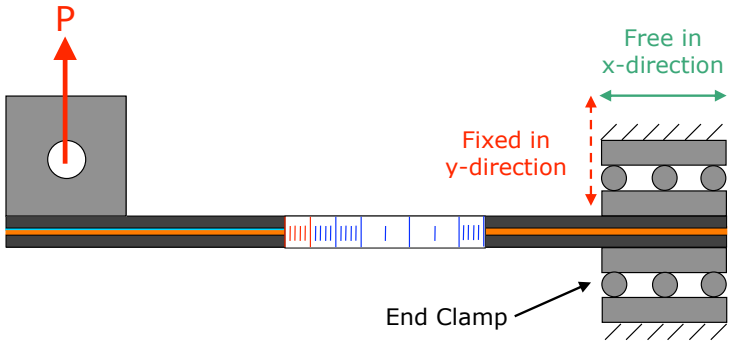

(a) FRMM illustration.

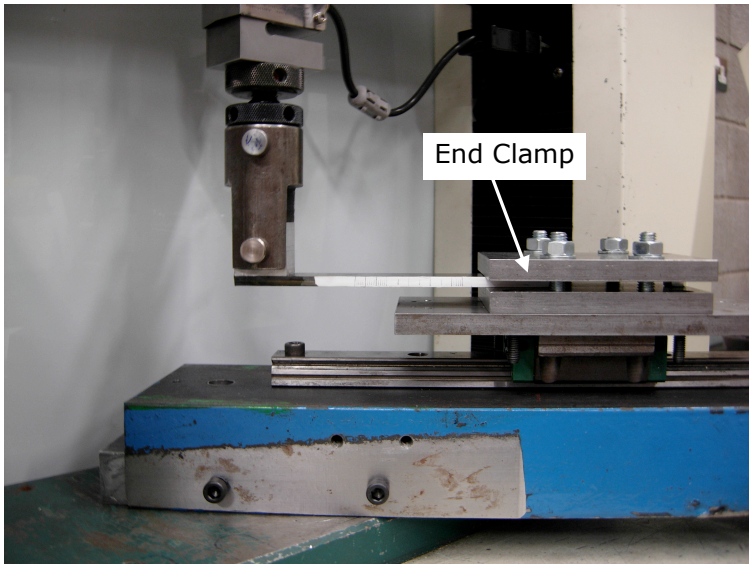

(b) FRMM photo.

Figure 2: Illustrations and photographs of FRMM experimental setups showing loading directions and fixtures used during testing.

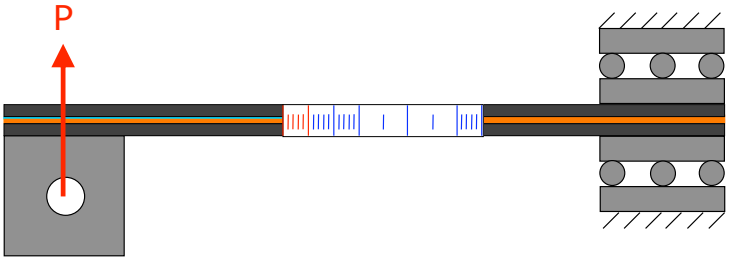

(a) ELS illustration.

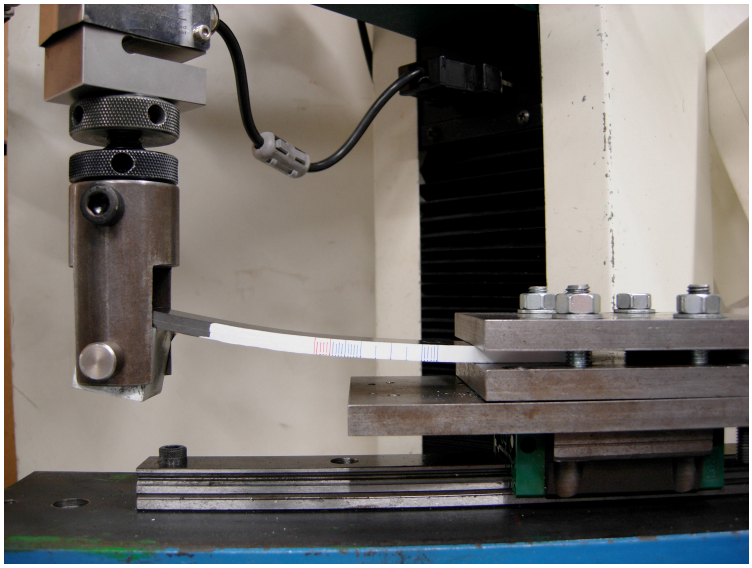

(b) ELS photo.

Figure 3: Illustrations and photographs of ELS experimental setups showing loading directions and fixtures used during testing.

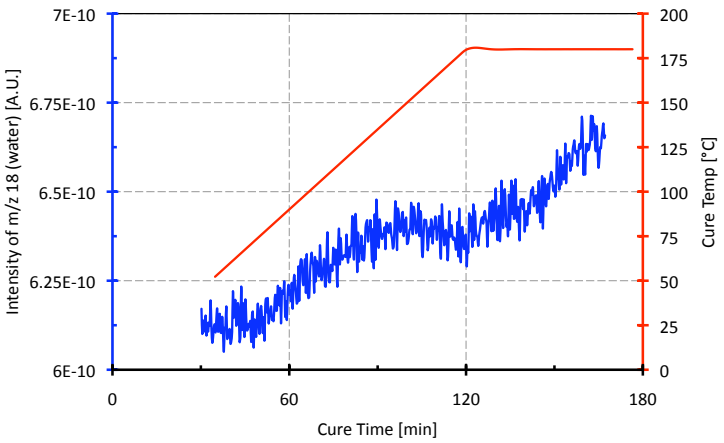

Figure 4: TGA-MS of water released from prepreg during the course of a cure cycle.

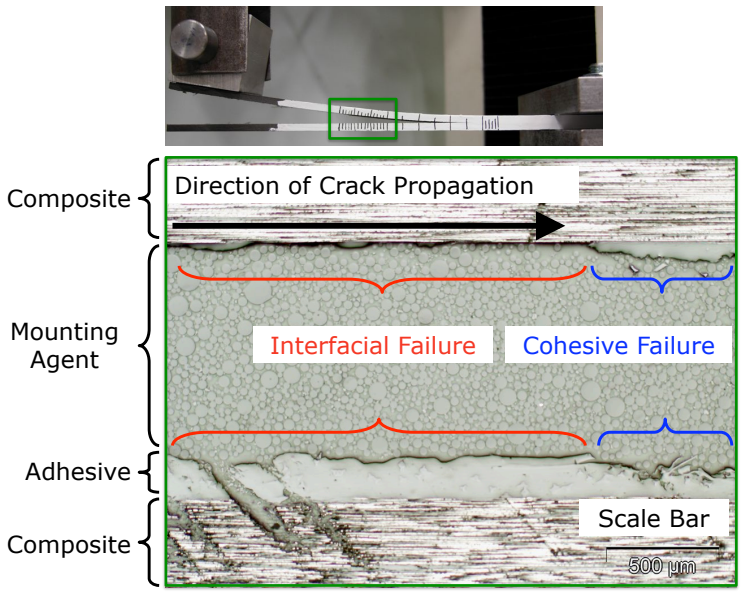

Figure 5: A typical sample prepared for optical microscopy after fracture testing.

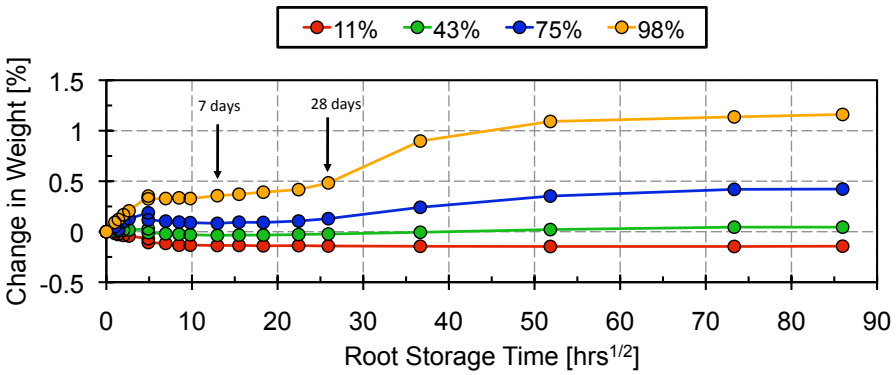

Figure 6: Weight variation of prepreg stored at various humidities over the course of 308 days. The points corresponding to 7 days (conditioning time before co-curing) and 28 days (shelf life of prepreg) are highlighted.

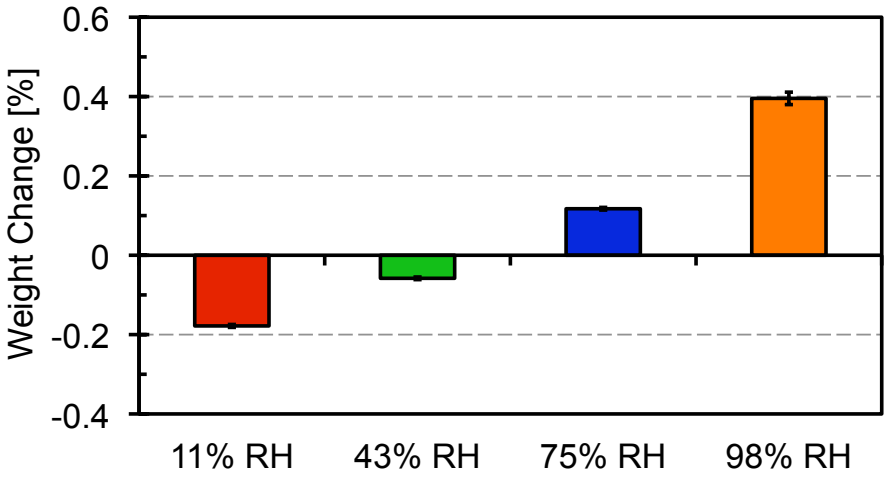

Figure 7: Weight variation of prepreg after 7 days at various humidity levels.

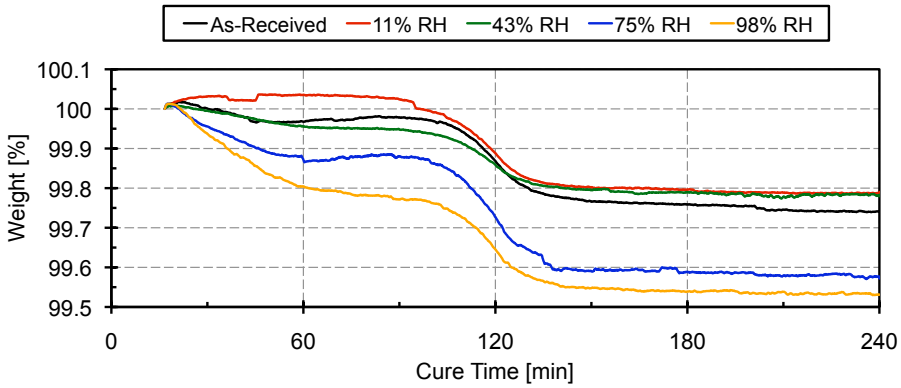

Figure 8: Weight loss trace of prepreg stored at various humidity levels during a simulated 180 °C cure cycle.

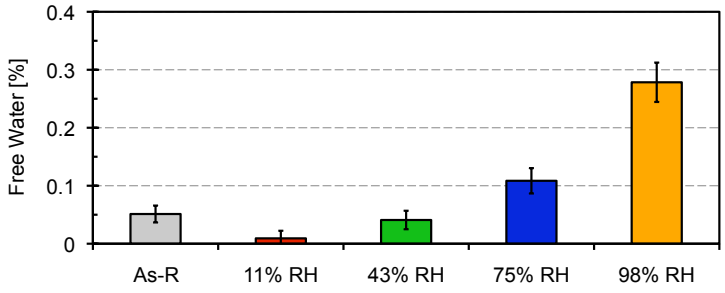

(a) Free Water

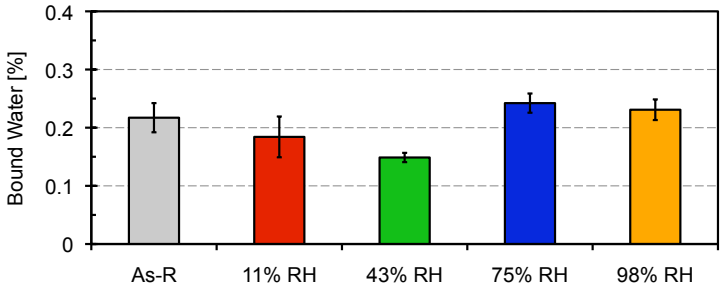

(b) Bound Water

Figure 9: Percentage of free and bound water stored in the prepreg as determined by TGA.

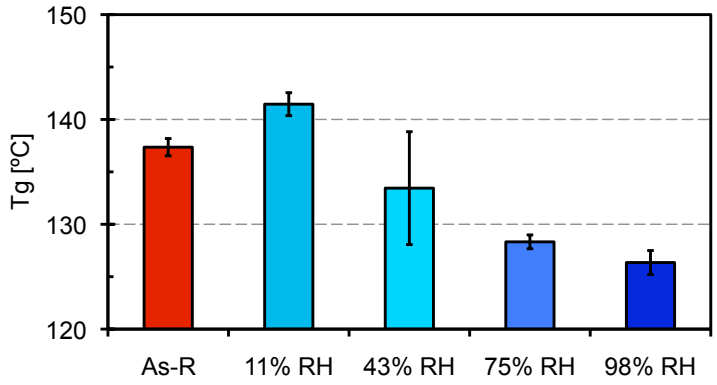

Figure 10: T_g of adhesive scrapings taken from fracture surface of co-cured joints.

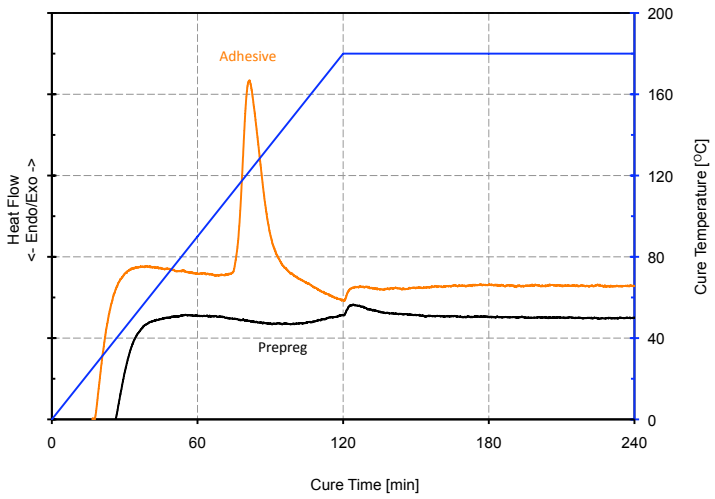

Figure 11: Heat flow of prepreg and adhesive over the course of a cure cycle.

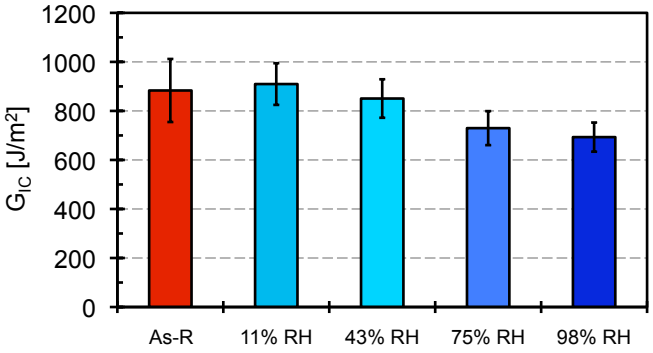

(a) DCB.

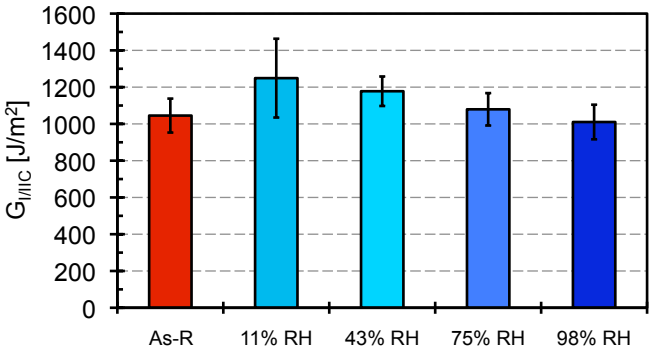

(b) FRMM.

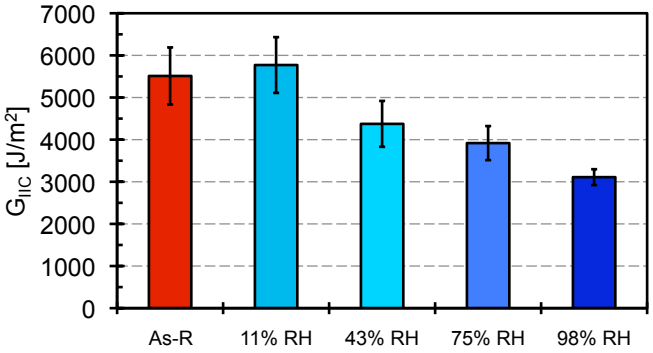

(c) ELS.

Figure 12: Fracture toughness of RH conditioned co-cured joints tested using DCB, FRMM & ELS geometries.

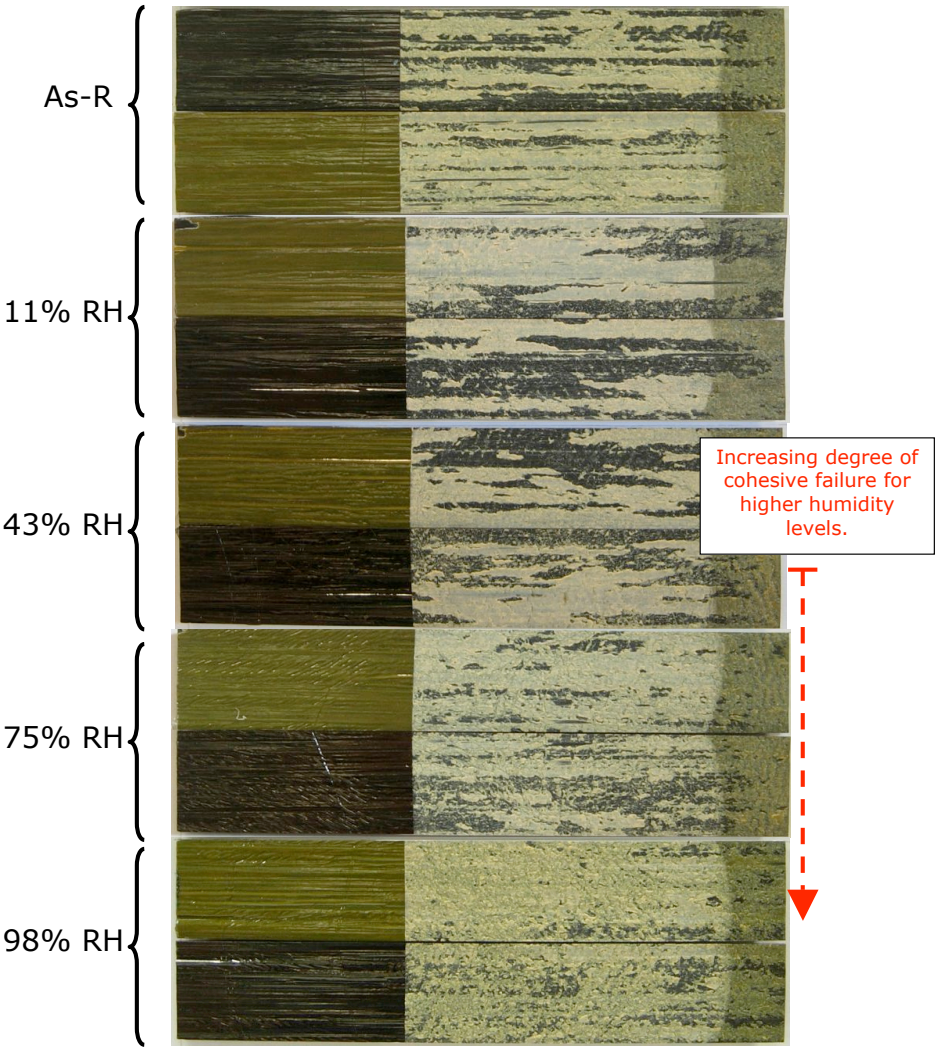

Figure 13: Fracture surfaces of Mode I DCB test.

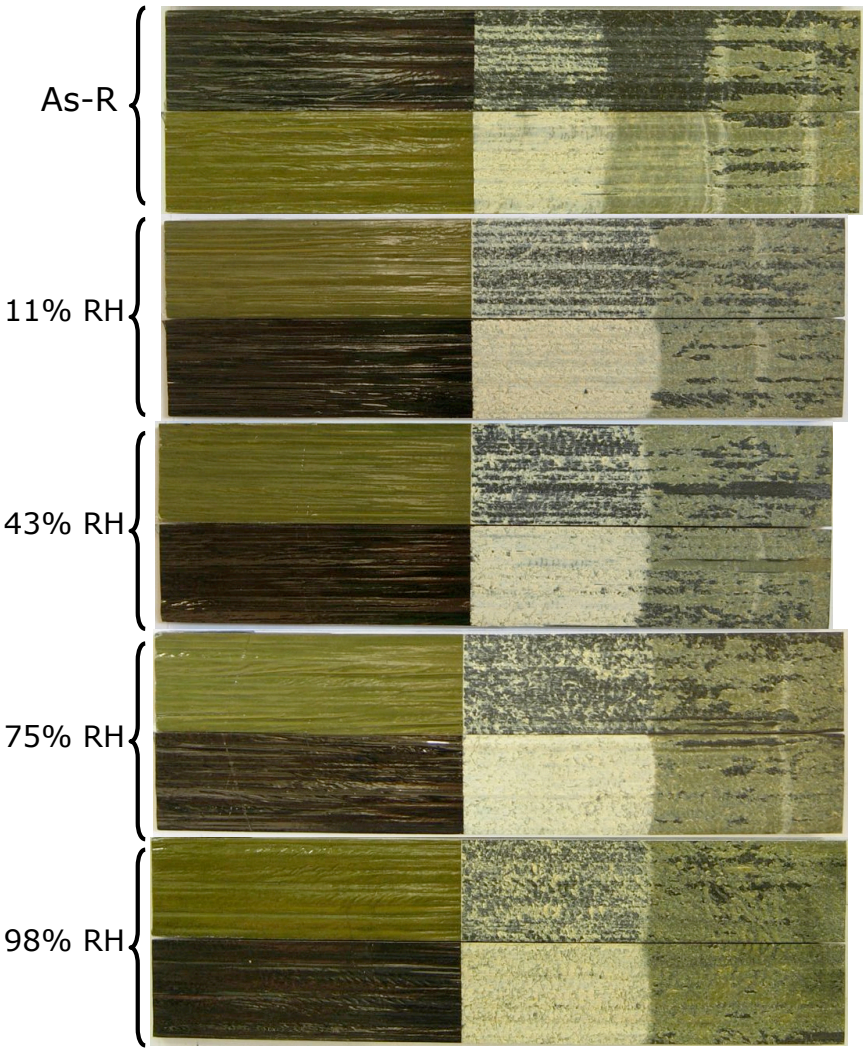

Figure 14: Fracture surfaces of Mixed Mode FRMM test.

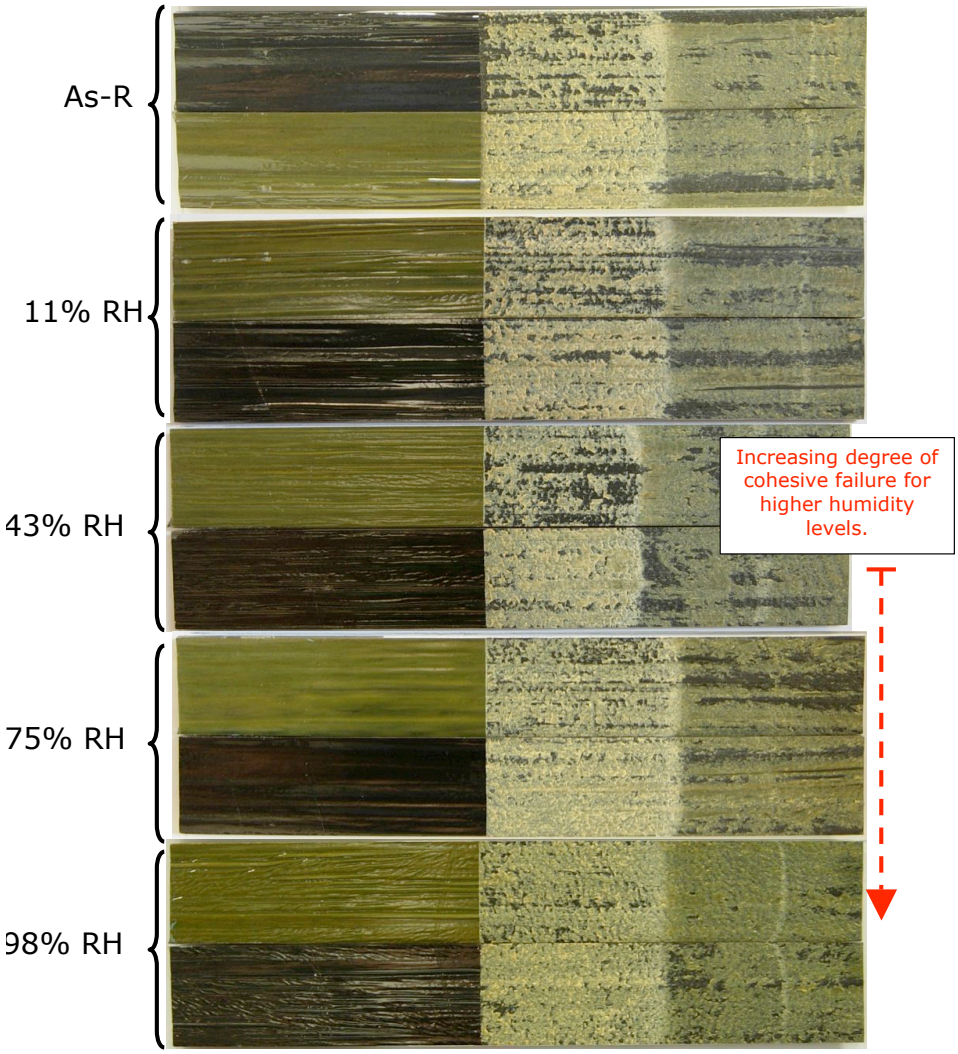

Figure 15: Fracture surfaces of Mode II ELS test.

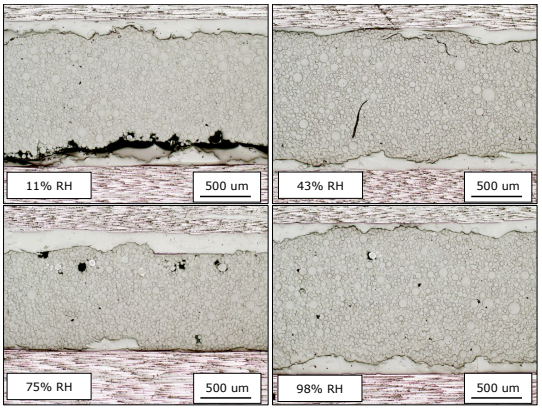

Figure 16: Crack path for RH conditioned co-cured joints tested using DCB.

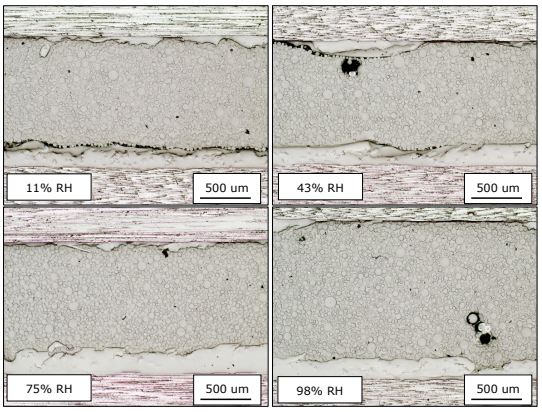

Figure 17: Crack path for RH conditioned co-cured joints tested using FRMM.

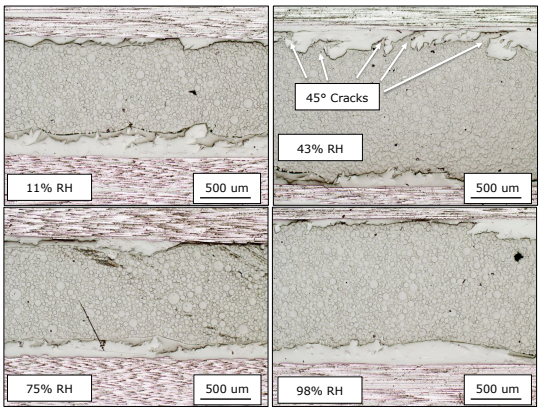

Figure 18: Crack path for RH conditioned co-cured joints tested using ELS.

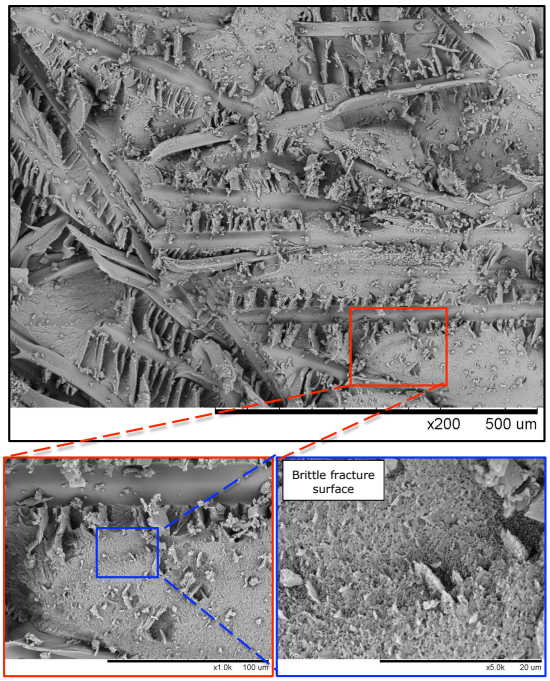

Figure 19: SEM image of fracture surface of co-cured joint conditioned at 11% RH and tested under mode II loading.

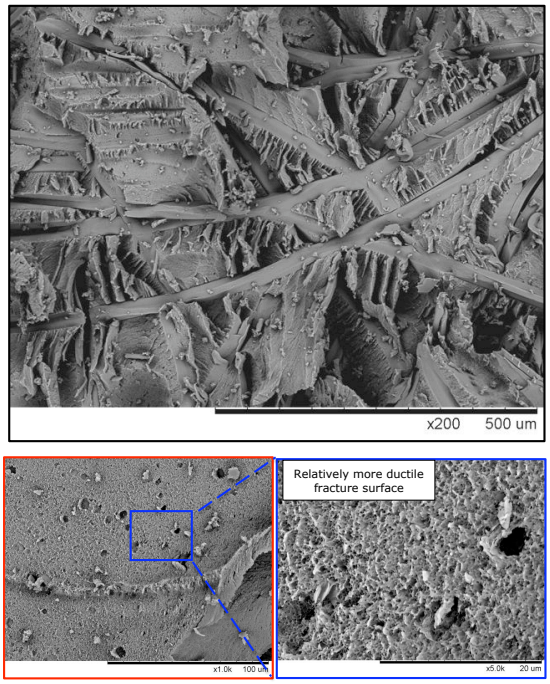

Figure 20: SEM image of fracture surface of co-cured joint conditioned at 98% RH and tested under mode II loading.

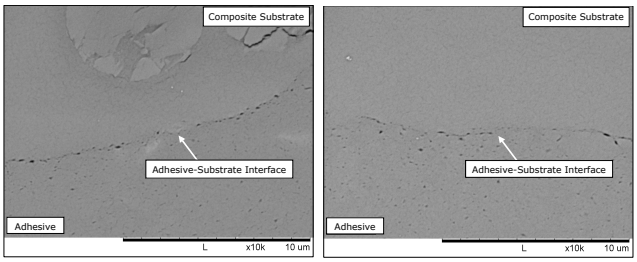

(a) 11% RH. (b) 43% RH.

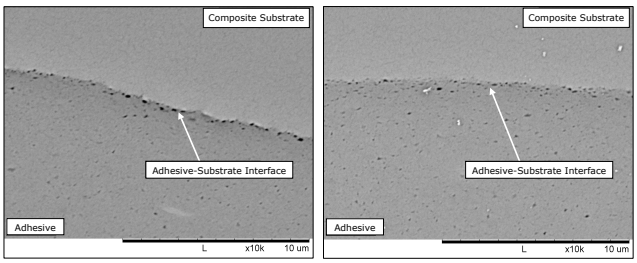

(c) 75% RH. (d) 98% RH.

Figure 21: SEM images of adhesive-substrate interface of co-cured joints manufactured from prepreg aged at various humidities for 1 week.